Al-Saigh et al. Nanoscale Research Letters (2018) 13:172
https://doi.org/10.1186/s11671-018-2587-1

Nanoscale Research Letters

NANO EXPRESS Open Access

Design of Strain-Engineered GeSn/GeSiSn Quantum Dots for Mid-IR Direct Bandgap Emission on Si Substrate

Reem Al-Saigh[1], Mourad Baira[2], Bassem Salem[3] and Bouraoui Ilahi[1*]

Abstract

Strain-engineered self-assembled GeSn/GeSiSn quantum dots in Ge matrix have been numerically investigated aiming to study their potentiality towards direct bandgap emission in the mid-IR range. The use of GeSiSn alloy as surrounding media for GeSn quantum dots (QD) allows adjusting the strain around the QD through the variation of Si and/or Sn composition. Accordingly, the lattice mismatch between the GeSn quantum dots and the GeSiSn surrounding layer has been tuned between − 2.3 and − 4.5% through the variation of the Sn barrier composition for different dome-shaped QD sizes. The obtained results show that the emission wavelength, fulfilling the specific QD directness criteria, can be successively tuned over a broad mid-IR range from 3 up to7 μm opening new perspectives for group IV laser sources fully integrated in Si photonic systems for sensing applications.

Keywords: GeSn, GeSiSn, Quantum dots, Direct bandgap, Mid-IR

Background

Recently, the demonstration of direct bandgap group IV materials through the alloying of Ge [1, 2] and SiGe [3, 4] with Tin has motivated intense research activities owing to the real and practically implementable opportunities towards photonics and electronics efficient on-chip integration. Indeed, GeSn alloy has been shown to exhibit direct bandgap beyond certain composition through the faster decrease of Γ compared to L valley [5–8]. While the reported results are very encouraging, the material properties and application potentialities are not yet fully explored. Indeed, the main actually available path to increase the operating wavelength of GeSn-based semiconductor lasers, towards the atmosphere transparency window that overlaps with absorbing lines of various gases [9], includes the increase of Sn content in the GeSn layers [10, 11]. However, because of the large lattice mismatch between Ge and Sn (14%), the preservation of the crystallographic quality of the material appears as the main challenge prohibiting this goal [12, 13]. A potentially interesting solution to increase the emission wavelength and ensure better carrier confinements relay on lower dimensional structures such as nanowires [14–16], nanorods [17], and quantum dots [18]. Within the specific directness criteria, the direct bandgap interband emission wavelength is theoretically limited to 4.3 μm [19]. To overcome these limitations, it is necessary to introduce an additional degree of freedom in the conception of group IV-based quantum structures. This can be ensured by using ternary GeSiSn layer [20–22], as a surrounding material for GeSn quantum dots (QD) offering the possibility of strain engineering by incorporating appropriate Si and Sn compositions. Accordingly, the use of GeSiSn strain engineering layer around GeSn QD is expected to offer a larger range of accessible direct bandgap emission wavelength.

In this context, we report on theoretical study of the effect of strain engineering by varying the Sn composition in the GeSiSn layer surrounding the GeSn QD on the direct bandgap interband emission wavelength.

Methods

Since the band offsets between binary and ternary Sn-containing group-IV alloys and Ge are not experimentally known, the relative band alignment between the different group-IV semiconductors involved in this work is evaluated, with respect to the valence band edge

* Correspondence: bilahi@ksu.edu.sa
[1]King Saud University Department of Physics and Astronomy, College of Sciences, Riyadh 11451, Saudi Arabia
Full list of author information is available at the end of the article

of Ge, using Jaros' simplified theory of band offsets [23] as detailed by D'Costa et al. [24]. The strain effects arising from the lattice mismatch between Ge substrate and GeSiSn layer and between the GeSn QD and the surrounding GeSiSn material have been evaluated for the conduction and valence band edges.

Indeed, the conduction band edge is shifted by δE_c^i and that of the valence band by δE_v as shown in Eq. (1) and (2):

$$\delta E_c^i = a_c^i\left(\varepsilon_{xx} + \varepsilon_{yy} + \varepsilon_{zz}\right) \quad (1)$$

$$\delta E_v = a_v\left(\varepsilon_{xx} + \varepsilon_{yy} + \varepsilon_{zz}\right) + b\left(\varepsilon_{xx} - \varepsilon_{zz}\right) \quad (2)$$

where i denotes L or Γ valley, a_c and a_v are the conduction and valence band deformation potential, respectively, and b is the shear deformation potential. $\varepsilon_{xx} = \varepsilon_{yy} = \varepsilon = \left(\frac{a_s - a_l}{a_l}\right)$ is the in-plan strain and $\varepsilon_{zz} = -2\frac{C_{12}}{C_{11}}\varepsilon_{xx}$ is the strain in the growth direction. a_s and a_l are respectively the lattice parameter of the substrate and the strained layer. C_{11} and C_{12} are the stiffness constants.

The binary and ternary alloy material parameters are derived from those of Ge, Si, and Sn by linear interpolation. These parameters are taken from Reference [11].

The composition-dependent strained bandgaps can be evaluated by adding the corresponding strain-generated energy shifts to the unstrained material's bandgap given in Eq. (3) for GeSn and Eq. (4) for GeSiSn:

$$E_g^i\left(\mathrm{Ge}_{1-X_d}\mathrm{Sn}_{X_d}\right) = (1-X_d)E_g^i(\mathrm{Ge}) + X_d E_g^i(\mathrm{Sn}) - b^i X_d(1-X_d) \quad (3)$$

$$E_g^i\left(\mathrm{Ge}_{1-x_b-y}\mathrm{Si}_y\mathrm{Sn}_{x_b}\right) = (1-x_b-y)E_g^i(\mathrm{Ge}) + x_b E_g^i(\mathrm{Sn}) + yE_g^i(\mathrm{Si}) - b^i_{\mathrm{GeSn}}x_b(1-x_b-y) - b^i_{\mathrm{SiSn}}y(1-x_b-y) - b^i_{\mathrm{GeSi}}x_b y \quad (4)$$

where b is the corresponding bandgap bowing parameter of the binary alloys summarized in Table 1.

To determine the carriers' confined states and deduce interband transition energies, the single-band effective mass Schrödinger equation has been solved in Cartesian coordinates by finite element method provided by COMSOL Multiphysics software [25]:

$$-\frac{\hbar^2}{2}\nabla\left(\frac{1}{m^*\left(\vec{r}\right)}\nabla\psi\left(\vec{r}\right)\right) + V\left(\vec{r}\right)\psi\left(\vec{r}\right) = E\psi\left(\vec{r}\right) \quad (5)$$

Table 1 Binary alloy's bandgap bowing parameters in eV

	b_{GeSn}	b_{GeSi}	b_{SiSn}
Γ (eV)	2.92 [31]	0.21 [32]	13.2 [33]
L (eV)	0.87 [31]	0.335 [32]	2.124 [32]

E represents the carrier's energy, and ψ is the corresponding wave function. m^* is the carrier's effective mass, $\hbar$ is the reduced Planck constant, $\vec{r}$ is the three-dimensional coordinate vector, and V is the carrier's confinement potential (band discontinuity). To simplify the calculation procedure of the QD electronic structure, we have adopted the constant strain approximation [26, 27] instead of the computationally expensive atomic simulation approach that obviously could give more precision in the strain distribution profile [28, 29]. Indeed, we consider the carriers confining potential in the compressively strained QD to be sufficiently deep to minimize the impact of the strain non-uniformity on the electron confined states [27]. Furthermore, the conduction band edges, which are the most important parameters in this work, allowing to study the bandgap directness, are only shifted by the hydrostatic strain being the less sensitive to the strain non-uniformity especially when a relatively low lattice mismatch is considered [30].

Results and Discussion

Since we are mainly concerned by the impact of the strain around the GeSn QD, the Sn composition of the QD is fixed at 28% and the Si composition of the GeSiSn at 35%; the study is therefore focused on the impact of the Sn barrier composition (x_b) variation between 6 and 22%. The resulting in-plan strain either in the GeSiSn layer or in the GeSn QD is given in Fig. 1a.

The in-plan strain in the two-dimensional layer of GeSiSn material varies between 0.6% ($x_b = 6\%$) and −1.7% ($x_b = 22\%$). We suppose that this layer remains pseudomeorphically strained allowing to keep the designed structure experimentally realizable. The GeSn is chosen to be compressively strained within the GeSiSn surrounding material with a lattice mismatch ranging from −2.3 to −4.5% ensuring favorable conditions to the formation of self-organized GeSn QD.

Figure 1b shows the dependence of the strained bandgap at L and Γ points from $\mathrm{Ge}_{0.72}\mathrm{Sn}_{0.28}$ and $\mathrm{Ge}_{(0.65-xb)}\mathrm{Si}_{0.35}\mathrm{Sn}_{xb}$ as a function of x_b. The Γ valley of $\mathrm{Ge}_{0.72}\mathrm{Sn}_{0.28}$ material remains below the L valleys, testifying its type I for the whole investigated range of tin barrier composition. Meanwhile, when the electron confinement is taken into account, the effective bandgap increases and the QD size effect becomes decisive [18] especially for highly strained QD. Indeed, in the presence of quantum confinement, the ground state energy should be considered instead of the minimum of the Γ band. Accordingly, smaller size QD are expected to have higher confined energy levels in the Γ valley that may exceed the L valley (and/or ground state electron energy level in the L valley). So, it is important to investigate the QD size's range obeying the specific directness criteria.

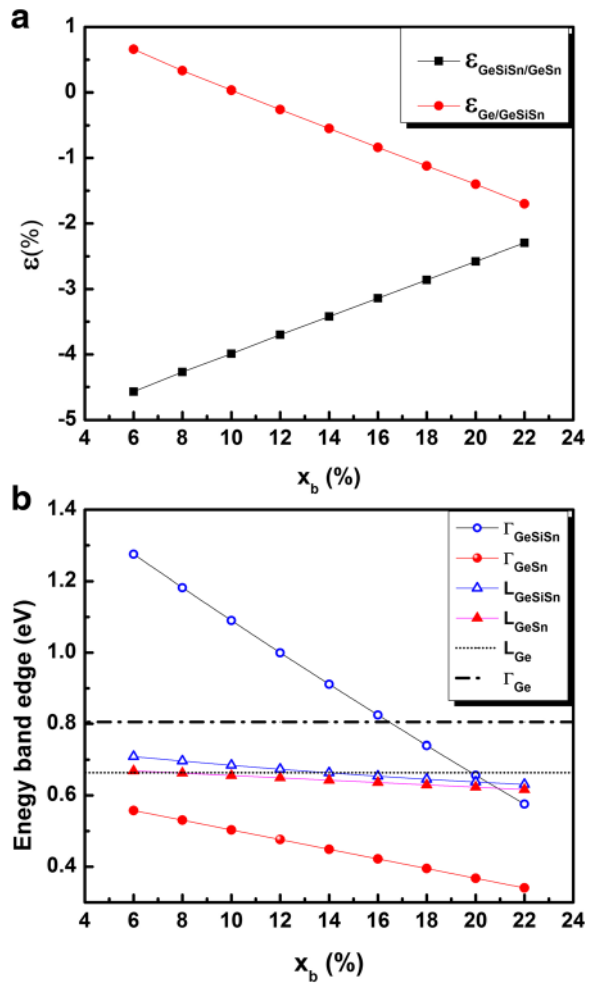

Fig. 1 a Lattice mismatch between $Ge_{0.65-xb}Si_{0.35}Sn_{xb}$ and Ge (filled circles) and between $Ge_{0.72}Sn_{0.28}$ and $Ge_{0.65-xb}Si_{0.35}Sn_{xb}$ (filled squares) as a function of x_b. **b** Band edges at L and G valleys for $Ge_{0.65-xb}Si_{0.35}Sn_{xb}$, $Ge_{0.72}Sn_{0.28}$, and Ge as a function of x_b

The modeled structure is schematically presented in Fig. 2. The $Ge_{0.72}Sn_{0.28}$ QD is considered to have a dome shape with a circular base of diameter D ranging from 15 to 40 nm and fixed height to diameter ratio equal to 0.25. The QD is positioned inside 15-nm-thick GeSiSn layer having a Si composition of 35% and a tunable Sn composition. This structure is supposed to be formed on Ge-buffered substrate and capped with Ge layer.

To ensure consistent QD design for better light-emitting device operation, a suitable directness parameter taking into the energy spacing between the lowest QD confined energy level position in L and G valleys has been introduced [18]. This parameter is denoted by GS_L-GS_Γ and should be higher than the room temperature thermal energy to avoid carriers' loss by thermal activation, where $GS_L(GS_\Gamma)$ represents the electron ground state energy level in the L valley (Γ valley) with respect the valence band maximum. The evaluation of GS_L-GS_Γ is schematically illustrated in the inset of Fig. 3.

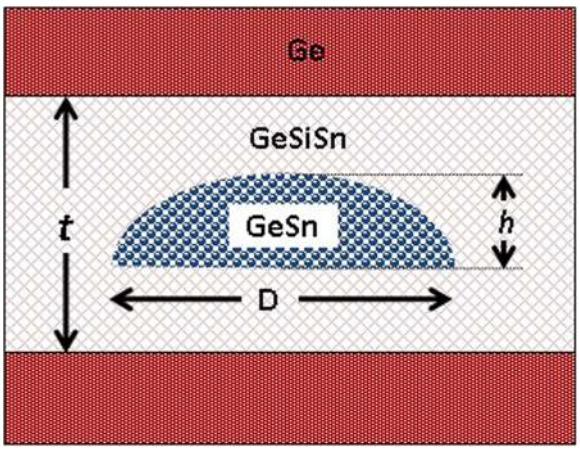

Fig. 2 Schematic presentation of the modeled GeSn QD of height (h) and diameter (D) within GeSiSn strain-reducing layer in Ge matrix

The calculation of the GeSn QD electron energy levels in Γ and L valleys for different diameters as a function of the Sn composition in GeSiSn allows to obtain the corresponding directness parameter (GS_L-GS_Γ). The results are plotted in Fig. 3. For a given x_b, the value of GS_L-GS_Γ is mainly governed by the QD size. Accordingly, the smaller dots having obviously higher confined energy states require lower bandgap energy through strain reducing to fulfill the directness criteria. As shown by Fig. 3, bigger dots ($D > 25$ nm) satisfy GSL-$GS_\Gamma > 26$ meV for x_b higher than 8%. However, efficient direct bandgap from small-size QD is found to be ensured for higher values of x_b ($x_b \geq 14\%$ for $D = 15$ nm).

Within the adopted parameters in this work, and especially the binary materials' bowing parameters, the

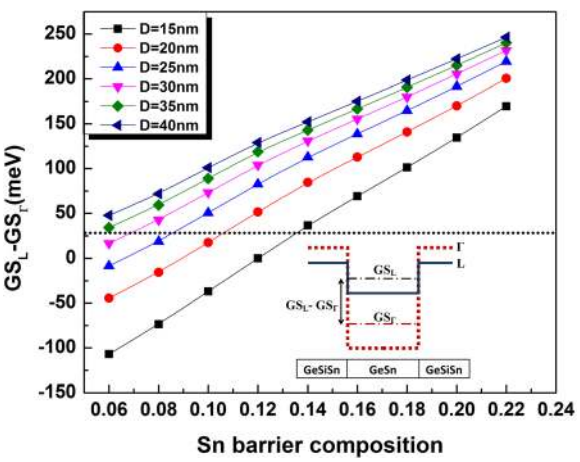

Fig. 3 Directness parameter (GS_L-GS_Γ) variation as a function of the $Ge_{0.72}Sn_{0.28}$ QD size and Sn composition of the $Ge_{0.65-x}Si_{0.35}Sn_x$ surrounding layer. The dotted line indicates the thermal energy at room temperature. The inset represents a schematic definition of the directness parameter

increase of the Sn content of the GeSiSn material reduces the stain around the QD and reduces also the surrounding material bandgap. Indeed, as shown in Fig. 1b, the increase of x_b from 6 to 22% reduces the conduction band discontinuity at Γ valley from 0.72 eV down to 0.23 eV. Indeed, as shown in Fig. 4, where the squared wave function $|\psi(\vec{r})|^2$ of the ground state electron in quantum dots of diameter 35 nm is shown in the xy plan for Sn barrier composition of 6% and 22%, the electrons are found to be fully localized inside the QD regardless of the barrier composition (conduction band's discontinuity). The strongly confined electrons indicate higher reliability of the investigated QD as an active medium for light emitters on Si substrate.

By limiting the QD sizes for a given x_b to those engendering efficient direct bandgap emission, we have appraised the QD ground state interband emission wavelength. The results are shown the Fig. 5, where the emission wavelength is plotted against x_b for different QD sizes. It is worth noting that the biggest QD size considered in this work ($D = 40$ nm) has shown small energy separation between the electron ground state and first excited state (below 26 meV) and has therefore been ignored from this study. Nonetheless, the evaluated emission wavelength as a function of x_b has been kept in Fig. 5 with a dotted line.

The wavelength range projected to be covered by the proposed QD design ranges from 3 up to 7 μm. The yielded range is extremely important for gas sensing application. The experimental implementation of this structure could offer the opportunity to cover, for the first time, the whole mid-IR range with a fully compatible material with existing microelectronic technology paving the way to new perspectives in CMOS compatible QD based mid-IR optoelectronics.

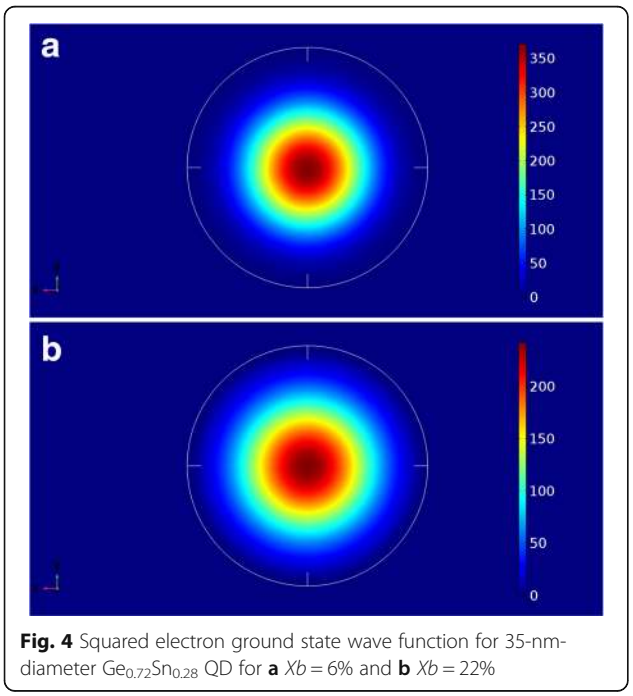

Fig. 4 Squared electron ground state wave function for 35-nm-diameter $Ge_{0.72}Sn_{0.28}$ QD for **a** $Xb = 6\%$ and **b** $Xb = 22\%$

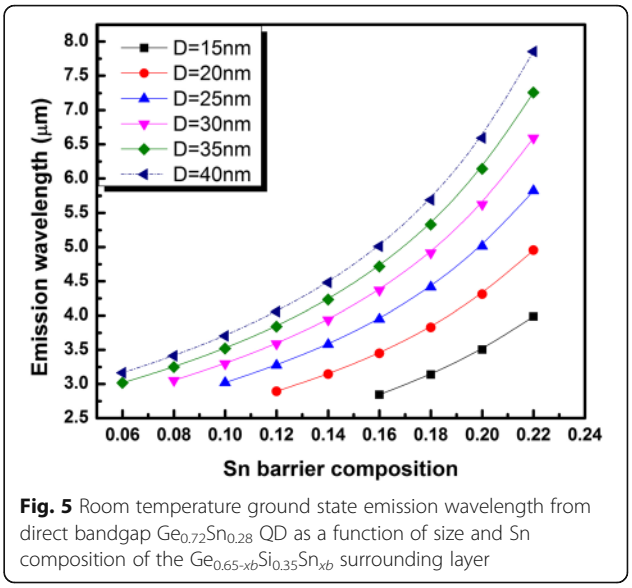

Fig. 5 Room temperature ground state emission wavelength from direct bandgap $Ge_{0.72}Sn_{0.28}$ QD as a function of size and Sn composition of the $Ge_{0.65-xb}Si_{0.35}Sn_{xb}$ surrounding layer

Conclusions

GeSn QD in GeSiSn strain engineering layer on Ge matrix have been investigated as a function of QD size and the lattice mismatch with surrounding material. Reducing the strain around the GeSn QD by varying the Sn composition of GeSiSn barrier material is found to enhance the direct bandgap type I emission wavelength from 3 up to 7 μm. The designed structure opens new perspectives in mid-IR light emitter fully compatible with Si technology.

Abbreviations

CMOS: Complementary metal-oxide-semiconductor; GS_L: Ground state electron level in L valley; $GS_Γ$: Ground state electron level in Γ valley; QD: Quantum dots

Acknowledgements

The author would like to thank the Deanship of Scientific Research at King Saud University for funding this work through the Research Project No R17-03-53.

Availability of Data and Materials

All data are fully available without restriction.

Authors' Contributions

MB and RA performed the calculations and data collection and drafted the manuscript. BS conducted the result evaluation and analyses and commented the manuscript. BI conceived and supervised the project and modified/edited the manuscript. All authors read and approved the final manuscript.

Authors' Information

RS is an Assistant Professor at the Department of Physics and Astronomy, College of Sciences, King Saud University.
MB is an Assistant Professor of Physics at the Higher Institute of Computer Sciences and Mathematics of Monastir and member of the Laboratory of

Micro-Optoelectronic and Nanostructures University of Monastir, Faculty of Sciences, University of Monastir, Tunisia.
BS is an Associate Researcher at the Microelectronics Technology Laboratory and the Nanomaterials' Research Group leader at Univ. de Grenoble Alpes, CNRS, CEA/LETI Minatec, Grenoble, France.
BI is an Associate Professor at the Department of Physics and Astronomy, College of Sciences, King Saud University.

Competing Interests
The authors declare that they have no competing interests.

Publisher's Note

Author details
[1]King Saud University Department of Physics and Astronomy, College of Sciences, Riyadh 11451, Saudi Arabia. [2]University of Monastir Faculty of Sciences, Laboratory of Micro-Optoelectronic and Nanostructures, 5019 Monastir, Tunisia. [3]Univ. de Grenoble Alpes, CNRS, CEA/LETI Minatec, LTM, F-38000 Grenoble, France.

Received: 18 January 2018 Accepted: 29 May 2018
Published online: 07 June 2018

References
1. He G, Atwater H (1997) Interband transitions in SnxGe1−x alloys. Phys Rev Lett 79:1937–1940 https://doi.org/10.1103/PhysRevLett.79.1937
2. Yin W-J, Gong X-G, Wei S-H (2008) Origin of the unusually large band-gap bowing and the breakdown of the band-edge distribution rule in the SnxGe1−x alloys. Phys Rev B 78:161203 https://doi.org/10.1103/PhysRevB.78.161203
3. Soref RA, Perry CH (1991) Predirect bandgap of the new semiconductor SiGeSn. J Appl Phys 69(1):539–541 http://dx.doi.org/10.1063/1.347704
4. Moontragoon P, Ikonić Z, Harrison P (2007) Band structure calculation of Si-Ge-Sn alloys: achieving direct bandgap materials. Semicond Sci Technol 22(7):742 http://dx.doi.org/10.1088/0268-1242/22/7/012
5. Low KL, Yang Y, Han G, Fan W, Yeo Y-C (2012) Electronic band structure and effective mass parameters of Ge1-xSnx alloys. J Appl Phys 112:103715. https://doi.org/10.1063/1.4767381
6. Gupta S, Magyari-Köpe B, Nishi Y, Saraswat KC (2013) Achieving direct band gap in germanium through integration of Sn alloying and external strain. J Appl Phys 113(7):073707
7. D'Costa VR, Cook CS, Birdwell AG, Littler CL, Canonico M, Zollner S, Kouvetakis J, Menendez J (2006) Optical critical points of thin-film Ge1−ySny alloys: a comparative Ge1−ySny/Ge1−xSix study. Phys Rev B 73(12):125207
8. Chen R, Lin H, Huo Y, Hitzman C, Kamins TI, Harris JS (2011) Increased photoluminescence of strain-reduced, high-Sn composition Ge1−xSnx alloys grown by molecular beam epitaxy. Appl Phys Lett 99(18):181125
9. Hodgkinson J, Tatam RP (2013) Optical gas sensing: a review. Meas Sci Technol 24:012004. https://doi.org/10.1088/0957-0233/24/1/012004
10. Gassenq A, Milord L, Aubin J, Guilloy K, Tardif S, Pauc N, Rothman J, Chelnokov A, Hartmann JM, Reboud V, Calvo V (2016) Gamma bandgap determination in pseudomeorphic GeSn layers grown on Ge with up to 15% Sn content. Appl Phys Lett 109:242107 https://doi.org/10.1063/1.4971397
11. Chang GE, Chang SW, Chuang SL (2010) Strain-balanced GezSn1−z–SixGeySn1−x−y multiple-quantum-well lasers. IEEE Journal of Quantum Electronics 46(12):1813. https://doi.org/10.1109/JQE.2010.2059000
12. Reboud V, Gassenq A, Pauc N, Aubin J, Milord L, Thai QM, Bertrand M, Guilloy K, Rouchon D, Rothman J, Zabel T, Armand Pilon F, Sigg H, Chelnokov A, Hartmann JM, Calvo V (2017) Optically pumped GeSn micro-disks with 16% Sn lasing at 3.1 μm up to 180 K. Appl Phys Lett 111:092101. https://doi.org/10.1063/1.5000353
13. Dou W, Benamara M, Mosleh A, Margetis J, Grant P, Zhou Y, Al-Kabi S, Du W, Tolle J, Li B, Mortazavi M, Yu S-Q (2018) Investigation of GeSn Strain Relaxation and Spontaneous Composition Gradient for Low-Defect and High-Sn Alloy Growth, Scientific Reports 8:5640. https://doi.org/10.1038/s41598-018-24018-6
14. Haffner T, Zeghouane M, Bassani F, Gentile P, Gassenq A, Chouchane F, Pauc N, Martinez E, Robin E, David S, Baron T, Salem B (2018) Growth of $Ge_{1-x}Sn_x$ Nanowires by chemical vapor deposition via vapor–liquid–solid mechanism using GeH_4 and $SnCl_4$. Phys. Status Solidi A 215:1700743. https://doi.org/10.1002/pssa.201700743
15. Biswas S, Doherty J, Saladukha D, Ramasse Qn, Majumdar D, Upmanyu M, Singha A, Ochalski T, Morris MA, Holmes JD (2016) Non-equilibrium induction of tin in germanium: towards direct bandgap Ge1−xSnx nanowires. Nat Commun 7:11405. https://doi.org/10.1038/ncomms11405
16. Assali S, Dijkstra A, Li A, Koelling S, Verheijen MA, Gagliano L, von den Driesch N, Buca D, Koenraad PM, Haverkort JEM, Bakkers EPAM (2017) Growth and Optical Properties of Direct Band Gap Ge/Ge0.87Sn0.13Core/Shell Nanowire Arrays, Nano Lett 17(3):1538–1544. https://doi.org/10.1021/acs.nanolett.6b04627
17. Seifner MS, Hernandez S, Bernardi J, Romano-Rodriguez A, Barth S (2017) Pushing the composition limit of anisotropic Ge1−xSnx nanostructures and determination of their thermal stability. Chemistry of Materials 29(22):9802–9813. https://doi.org/10.1021/acs.chemmater.7b03969
18. Ilahi B (2017) Design of direct band gap type I GeSn/Ge quantum dots for mid-IR light emitters on Si substrate. Physica Status Solidi RRL 11(5):1700047. https://doi.org/10.1002/pssr.201700047
19. Baira M, Salem B, Madhar NA, Ilahi B (2018) Tuning direct bandgap GeSn/Ge quantum dots' interband and intraband useful emission wavelength: towards CMOS compatible infrared optical devices. Superlattice Microst 117:31–35 https://doi.org/10.1016/j.spmi.2018.02.038
20. Soref RA, Kouvetakis J, Menendez J (2007) Advances in SiGeSn/Ge technology. Mater Res Soc Symp Proc 958:0958L
21. Jiang L, Xu C, Gallagher JD, Favaro R, Aoki T, Menéndez J, Kouvetakis J (2014) Development of light emitting group IV ternary alloys on Si platforms for long wavelength optoelectronic applications. Chem Mater 26(8):2522–2531. https://doi.org/10.1021/cm403801b
22. Wirths S, Buca D, Ikonic Z, Harrison P, Tiedemann AT, Holländer B, Stoica T, Mussler G, Breuer U, Hartmann JM, Grützmacher D, Mantl S (2014) SiGeSn growth studies using reduced pressure chemical vapor deposition towards optoelectronic applications. Thin Solid Films 557:183–187 https://doi.org/10.1016/j.tsf.2013.10.078
23. Jaros M (1988) Simple analytic model for heterojunction band offsets. Phys Rev B 37:7112–7114 https://doi.org/10.1103/PhysRevB.37.7112
24. D'Costa VR, Fang Y-Y, Tolle J, Kouvetakis J, Menéndez J (2010) Ternary GeSiSn alloys: new opportunities for strain and band gap engineering using group-IV semiconductors. Thin Solid Films 518:2531
25. Melnik RVN, Willatzen M (2004) Bandstructures of conical quantum dots with wetting layers. Nanotechnology 15(1) https://doi.org/10.1088/0957-4484/15/1/001
26. Souaf M, Baira M, Nasr O, Alouane MHH, Maaref H, Sfaxi L, Ilahi B (2015) Investigation of the InAs/GaAs quantum dots' size: dependence on the strain reducing layer's position. Materials 8:4699–4709 https://doi.org/10.3390/ma8084699
27. Chen J, Fan WJ, Zhang DH, Xu Q, Zhang XW (2013) Electronic structure of Ge/SixSnyGe1−x−y quantum dots, Nanoelectronics Conference (INEC), IEEE 5th International, Singapore. https://doi.org/10.1109/INEC.2013.6466071
28. Ilatikhameneh H, Ameen TA, Klimeck G, Rahman R (2016) Universal behavior of atomistic strain in self-assembled quantum dots. IEEE J Quantum Electron 52(7):1–8. https://doi.org/10.1109/JQE.2016.2573959
29. Pryor C, Kim J, Wang LW, Williamson AJ, Zunger A (1998) Comparison of two methods for describing the strain profiles in quantum dots. J Appl Phys 83:2548 https://doi.org/10.1063/1.366631
30. Tadić M, Peeters FM, Janssens KL, Korkusiński M, Hawrylak P (2002) Strain and band edges in single and coupled cylindrical InAs/GaAs and InP/InGaP self-assembled quantum dots. J Appl Phys 92:5819. https://doi.org/10.1063/1.1510167
31. Chibane Y, Ferhat M (2010) Electronic structure of SnxGe1−xSnxGe1−x alloys for small Sn compositions: unusual structural and electronic properties. J Appl Phys 107:053512 https://doi.org/10.1063/1.3326162
32. Moontragoon P, Soref RA, Ikonic Z (2012) The direct and indirect bandgaps of unstrained SixGe1−x−ySny and their photonic device applications. J Appl Phys 112:073106. https://doi.org/10.1063/1.4757414
33. D'Costa VR, Fang Y-Y, Tolle J, Kouvetakis J, Menéndez J (2009) Tunable optical gap at a fixed lattice constant in group-IV semiconductor alloys. Phys Rev Lett 102:107403 https://doi.org/10.1103/PhysRevLett.102.107403